Comparison of Backflashover Performance of a Fully Composite Pylon with Internal and External Grounding Down-leads

Zhang, Hanchi; Yin, Kai; Ghomi, Mohammad; Silva, Filipe Miguel Faria da; Bak, Claus Leth

Published in:
17th International Symposium on Lightning Protection, SIPDA 2023

DOI (link to publication from Publisher):
10.1109/SIPDA59763.2023.10349196

Publication date:
2023

Document Version
Accepted author manuscript, peer reviewed version

cigre SIPDA For power system expertise SUZHOU CHINA
CIGRE ICLPS - SIPDA
International Colloquium on Lightning and Power Systems
International Symposium on Lightning Protection
Oct 09 - 13, 2023

Comparison of Backflashover Performance of a Fully Composite Pylon with Internal and External Grounding Down-leads

Hanchi Zhang
AAU Energy
Aalborg University
Aalborg, Denmark
hazh@energy.aau.dk

Kai Yin
Department of Information and Electrical Engineering
Hangzhou City University
Hangzhou, China
yinkai@zucc.edu.cn

Mohammad Ghomi
AAU Energy
Aalborg University
Aalborg, Denmark
mgh@energy.aau.dk

Filipe Faria da Silva
AAU Energy
Aalborg University
Aalborg, Denmark
ffs@energy.aau.dk

Claus Leth Bak
AAU Energy
Aalborg University
Aalborg, Denmark
clb@energy.aau.dk

***Abstract*—Transmission towers made of composite material with aesthetic appearance are designed and proposed for the increasing installation of overhead lines. From the aspect of lightning protection, it is desirable to connect a grounding down-lead to bring the ground potential to the shield wires, either inside the hollow body of composite pylons or outside. This paper aims to compare the back flashover performance of these two grounding approaches. The mutual capacitances between the down-leads and phase conductors are simulated and calculated by FEM tools. A dynamic corona model is used to simulate the transient response of the down-leads. Without considering the corona, external down-lead has a slightly lower surge impedance and mutual capacitances, but the two grounding approaches give the close back flashover rates. It is stressed that the surge corona effect is necessary for modelling thin-wire grounding devices, otherwise, the back flashover rate can be overestimated by 20 % to 30 %. If the corona effect is considered, the back flashover rate provided by adopting internal down-leads is a bit higher, because the corona expansion can be hindered in the cross arm.**

***Keywords*—composite pylon, lightning protection, back flashover rate, corona effect, PSCAD**

I. INTRODUCTION

Catering to the green transition and increasing demand for electrical energy, more and more renewable power plants have been established, such as offshore wind farms. These power plants are generally located far away from both the load centres and the existing power grid [1]. Overhead lines can serve as an economic and practical solution to transmit plenty of electric power over long distances. However, public opinion is not satisfied with conventional steel lattice towers, because of their negative visual impact and large footing area. Facing the contradiction between the demands for new transmission lines and towers, and the opposition from the public, several more compact and aesthetic transmission pylons have been designed and proposed, as shown in Fig. 1 (a)-(d) [2-5]. In order to abandon the unpleasant appearance of conventional steel lattice towers, some of the novel pylons are manufactured with composite materials. In addition, the pylons made of composite materials possess economic advantages including lower costs of production, assembly, and maintenance. Furthermore, the components of the tower are easier to assemble and transport, and the construction period and cost are greatly reduced.

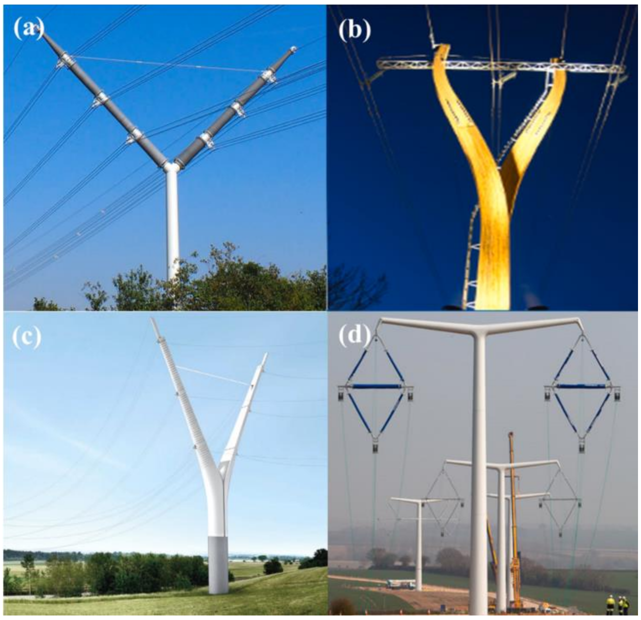

Fig.1 (a) The 'Y' shaped pylon proposed by the European Composite Pylon project[2]. (b) Finland tower [3]. (c) Y-Pylon proposed by Knight Architects with Roughan & O'Donavon, and ESB International in association with MEGA [4]. (d) Prototypes of 'T' pylon [5].

A common issue is that the pylons made of composite materials are totally insulated, so they cannot conduct lightning current if the shield wires clamped on them are struck by lightning. Naturally, it is desirable to connect a grounding down-lead to bring the ground potential to the shield wires. The shafts of the composite pylons are generally hollow, so a grounding down-lead installed inside the pylon shafts can be one option, while a bare conductor installed externally can be another. In order to assess and compare the back flashover performance of adopting these two grounding strategies, it is necessary to represent the transient response of internal and external down-leads accurately.

The transient representation of the grounding down-lead is generally parameterized into the unit inductance and unit capacitance of the down-leads in the analysing space. The mutual inductance of the down-lead to other conductors can be neglected because of their non-parallel relative positions. Hence, the inductance of the down-lead is mainly equal to its inductance-to-ground. Similarly, the capacitance can be classified into capacitance-to-ground and mutual capacitances to phase conductors. In this paper, the transient model of the grounding down-lead is represented by mutual capacitances to phase conductors and surge impedance. Mutual capacitances can be calculated accurately by Finite Element Method [6-8]. The surge impedance modelling transmission towers has been studied experimentally and theoretically for decades [9-13]. All these surge impedance models neglect the surge corona on the tower, because the corona sheath during a surge is relatively small compared to tower size and thus, its effect on tower transient response is small. However, the down-leads are quite thin with a cross-section radius of around 1 cm, which is comparable to the size of surge corona sheath. Therefore, the surge corona has a nonnegligible effect on the surge impedance of down-leads [14].

This paper aims to compare the back flashover performance of adopting the two grounding approaches, internal and external down-leads. A specific composite pylon, the Y-shaped pylon as shown in Fig. 1 (a) is selected as an example case. The modelling of the internal and external down-leads is highlighted first from the details of mutual capacitances to phase conductors, surge corona effect, and surge impedance, followed by other common simulating components. The corona developing processes are presented first and then, the effect on overvoltage and back flashover rate is analysed. It is pointed that the corona expansion around the internal down-lead is restricted by the cross arm.

II. Modelling of the Internal and External Grounding Down-leads

A. Mutual Parasitic Capacitance

Uni-body composite pylons eliminate the suspension insulators, resulting in a higher mutual parasitic capacitance between the down-lead and phase conductors compared with steel lattice towers. The value of parasitic capacitances depends on the geometric arrangement of the down-leads and phase conductors, so the values of internal and external down-leads are different and can be calculated by FEM [15]. In the equivalent circuit, the parasitic capacitances are represented by lumped capacitors connected between the down-leads and conductors whose arrangement can be demonstrated in the following Fig. 3. The values of the lumped mutual capacitances are listed in Table I, obtained with COMSOL. It can be found that because the distance of the internal down-lead to the phase conductors is shorter than from the external down-lead, the mutual parasitic capacitances between internal down-lead and phase conductors are larger.

TABLE I. The Mutual Parasitic Capacitances between Phase Conductors and Internal & External Grounding Down-leads

	Upper phase	**Middle phase**	**Lower phase**
Internal DL	91.22 pF	76.70 pF	74.62 pF
External DL	74.50 pF	53.76 pF	52.42 pF

B. Surge Corona Effect

As stated before, the surge corona has a nonnegligible effect on the surge impedance of thin-wire grounding devices. Thus, it is necessary to consider the corona effect in the transient representation of both internal and external down-leads. Corona discharge is represented by the increased capacitance of the down-lead.

For external down-leads, a dynamic corona radius model is adopted[14]. When overvoltage on the down-lead exceeds V_i, corona onsets. During expansion, corona radius $r_c(t)$ is restricted by both the expansion velocity v_c and the maximum expansion radius $r_{max}(t)$. When $t=t_f$, overvoltage reaches its crest and starts decreasing, corona starts shrinking at the shrinking velocity, which is numerically equal to 1 m/μs in this research. Thus, it can be described as equation (1), where t_0 is the time when $r_c(t_0)$ equals to r. As a result, the dynamic capacitance of the external down-lead can be calculated with dynamic corona radius, as shown in equation (2).

$$r_c(t) = \begin{cases} \min\{v_{cr} \cdot (t - T_g - t_{cr}), r_{max}(t)\}, \partial V/\partial t > 0 \\ r_{cr}(t_f) - v_{cr} \cdot (t - t_f), \partial V/\partial t < 0, t < t_0 \end{cases} \quad [\text{m}](1)$$

$$C = \frac{2\pi\varepsilon_0}{\ln(\frac{2\sqrt{2}h}{r + r_c(\text{t})}) - 1} \quad [\text{F/m}](2)$$

For internal down-leads in this specific case, [16] used experiments and simulations to conclude that after lightning overvoltage rises along the down-lead, the corona discharge may fill the entire cross arm and the capacitance of the down-lead will increase to a constant limit. The corona discharge will not occur outside the cross arm of the Y-shaped pylon unless the lightning current is stronger than 300 kA. The developing process for the corona from inception to fill the entire cross arm is ignored. The corona effect can be simply modelled as a switching capacitor with two values, geometry capacitance C_{geo} and corona capacitance C_{cor}, which can be evaluated in the following equations [17],

$$C_{geo} = \frac{2\pi\varepsilon_0}{\ln(\frac{2h}{r} - 1)} \quad [\text{F/m}](3)$$

$$C_{cor} = \frac{2\pi\varepsilon_0}{\ln(\frac{2h}{b} - 1)} \quad [\text{F/m}](4)$$

where ε_0 is the vacuum dielectric permittivity, h is the height of the center of each down-lead segment, r is the radius of the down-lead, and b is the inner radius of the cross arm. Then, the capacitance of the down-lead during a lightning surge can be represented as a piece-wise constant function as shown in equation (5)[16],

$$C = \begin{cases} C_{geo}, t < t_i + T_g \\ C_{cor}, V \geq V_i, \partial V/\partial t > 0, t > t_i + T_g \\ C_{geo}, \partial V/\partial t < 0, t > t_i + T_g \end{cases} \quad [\text{F/m}](5)$$

where V_i is the inception voltage for corona, t_i is the time when voltage exceeds Vi, T_g is the statistical time lag ranging from 0.4 μs to 0.8 μs. Corona only exists during the voltage-increasing stage ($\partial V/\partial t > 0$) and ceases when the voltage starts decreasing ($\partial V/\partial t < 0$).

Compared to the dynamic corona radius model, the switching capacitance model is not accurate enough. Thus, the dynamic corona radius model in equation (1) is modified to consider that the corona expansion can be hindered by the cross arm, as shown in equation (6),

$$r_c(t) = \begin{cases} \min\{v_{cr} \cdot (t - T_g - t_{cr}), r_{max}(t), b\}, \partial V/\partial t > 0 \\ r_{cr}(t_f) - v_{cr} \cdot (t - t_f), \partial V/\partial t < 0, t < t_0 \end{cases} \quad [\text{m}](6)$$

where the corona radius is also restricted by the inner radius of cross arm b.

The corona gradually decreases to zero along the conductor close to the ground [18]. Thus, the corona effect is not considered when simulating the vertical part of down-lead.

C. Surge Impedance

To consider the mutual parasitic capacitances between the down-lead to each phase conductor, the inclined part is divided into 4 segments. The joint of two adjacent segments is connected to a lumped capacitor simulating mutual parasitic capacitance as shown in Fig. 3. The bending and inclining segments are approximated into vertical and horizontal segments. The surge impedance of each segment is calculated by their unit inductance and capacitance in equation (7)[17].

$$Z = \sqrt{\frac{L}{C^*}} \quad [\Omega](7)$$

where the inductances L are calculated by equation (8)[17],

$$L = \frac{\mu_0}{2\pi} \cdot \left(\ln(\frac{2\sqrt{2}h}{r}) - 1 \right) \quad [\text{H/m}](8)$$

where μ_0 is the vacuum permeability and the capacitances C^* is the dynamic capacitance modelled by equation (5).

Neglecting corona effect, the surge impedance of internal and external down-leads is shown in Fig. 2 at different heights. It can be found the surge impedance of external down-lead is always smaller than that of the internal down-lead.

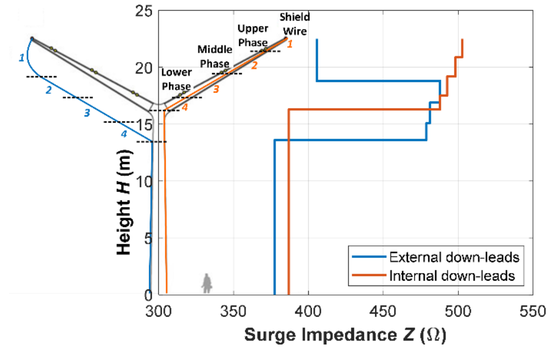

Fig.2 The constant surge impedance of each segment on internal and external down-leads at different height.

D. Other Modelling Components and Backflashover Evaluation Procedure

Except the modelling of internal and external down-leads, all the other modelling components and back flashover evaluation procedure are identical for both grounding strategies. The simulation is implemented in PSCAD.

The pylon footing is modelled considering its frequency-dependence [19]. A single-layer soil with resistivity ρ of 100 Ω·m is assumed.

The flashover is determined by leader progression model [20]. Only the flashover between the tip of the down-leads and the upper phase conductor is simulated.

The back flashover rate (BFR) is calculated by the statistical model after evaluating the critical lightning current [21]. Details of performing the simulating models and estimating BFR can be found in [22].

The important simulating components on the composite pylon with down-leads and how they are arranged are demonstrated in the following Fig.3.

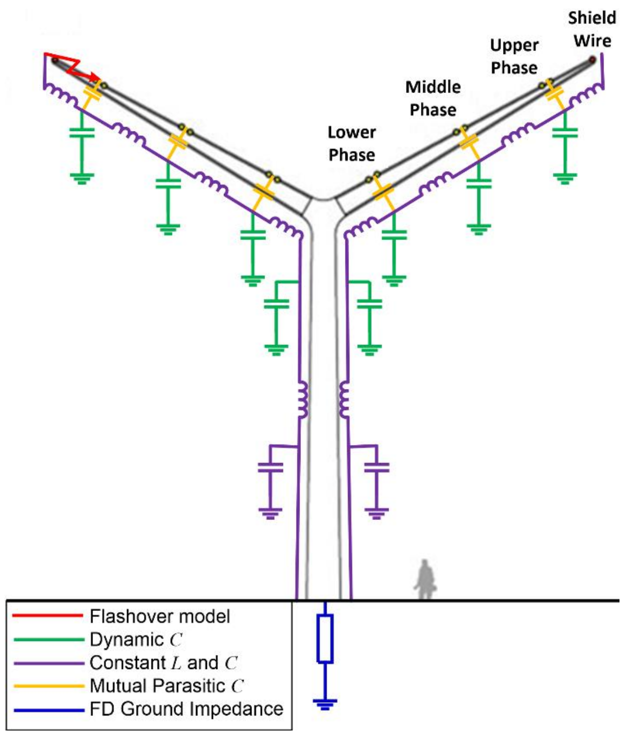

Fig.3 The demonstration of the important simulating components on the composite pylon with down-leads.

III. Results

A. Corona Developing Processes on Internal and External Down-leads

The corona developing processes around every segment of the internal and external down-leads are simulated and shown in the following Fig. 4. It can be found that the corona development consists of three stages. The first stage is dominated by the expansion velocity v_c first when the overvoltage exceeds the corona inception voltage V_i. The second is dominated by the maximum expansion radius until the overvoltage reaches crest and starts decreasing. Then the third stage is dominated by the shrinking velocity.

Three lightning current crest values, 60 kA, 100 kA, and 140 kA, are selected to illustrate the difference of corona development on the internal and external down-leads. When lightning current is low (60 kA), the corona on the internal and external down-leads develops in almost the same trend. When lightning current crest increases to 100 kA, the corona on the external down-lead can develop freely, whereas the corona radius around the Segment 1 of the internal down-lead reaches the inner radius of the cross arm (0.157 m), which hinders further expansion of corona. Furthermore, if the lightning current crest continues increasing to 140 kA, the corona on the external down-lead can still develop freely, but the corona on both Segment 1 and Segment 2 of the internal down-lead is hindered by the cross arm.

As analysed above, thicker corona sheath can reduce the surge impedance of the grounding down-leads. The barrier to corona development in the internal download means that the effect of corona on decreasing overvoltage is also impaired.

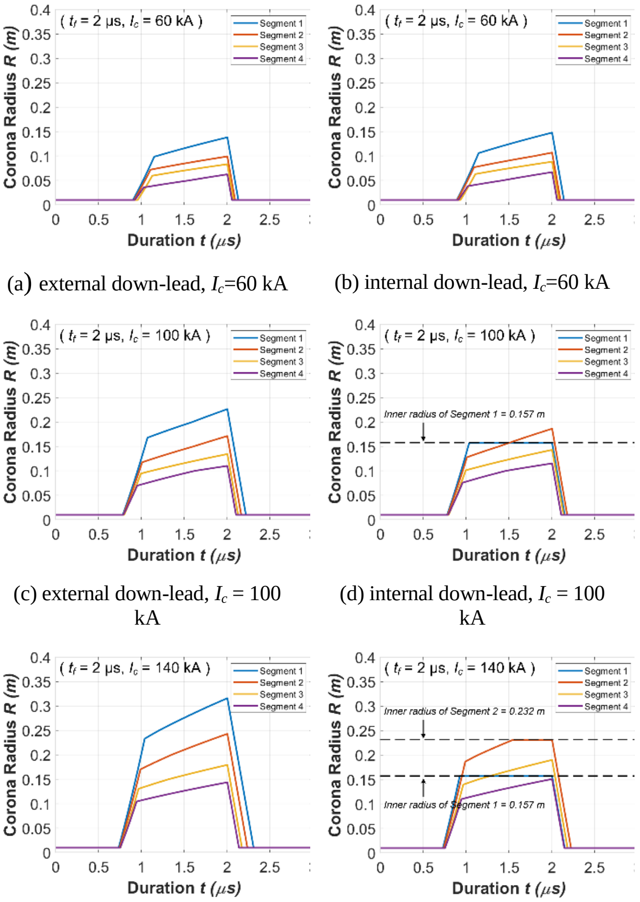

(a) external down-lead, I_c=60 kA (b) internal down-lead, I_c=60 kA

(c) external down-lead, I_c = 100 kA (d) internal down-lead, I_c = 100 kA

(e) external down-lead, I_c = 140 kA (f) internal down-lead, I_c = 140 kA

Fig. 4 Corona developing processes on external down-lead (a) (c) (e) and internal down-lead (b) (d) (f) under different lightning current crests.

B. *Overvoltage Level of Installing Internal and External Down-leads*

The overvoltage levels at the highest down-lead segments under the lightning currents with the same front time (2 μs) and different current crests are recorded. The differences of overvoltage created by the down-leads with/without corona effect are also shown in Fig. 5. The overvoltage levels provided by down-lead models without considering corona effect are shown in dashed curves, while the overvoltage levels provided by down-lead models considering corona effect are shown in solid curves.

If the corona effect is not considered, the overvoltage levels created by internal down-lead and external down-lead are almost equal. The largest difference is for a 200-kA lightning current and still less than 0.2 %. The overall surge impedance of the external down-lead is slightly lower than that of the internal down-lead, so the overvoltage resulted from a lower surge impedance reaches a little lower amplitude. However, the coupling capacitances of the external down-lead are smaller than those of the internal down-lead, which shall increase overvoltage. As a result of the two factors, the overvoltage level of the external down-leads is a little higher than that of the internal down-lead.

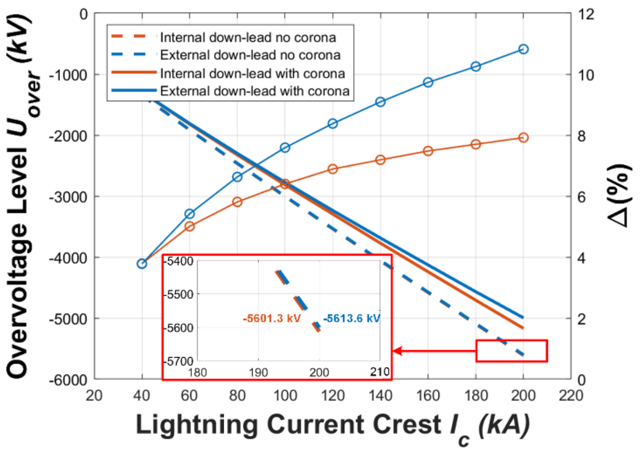

Fig. 5 Overvoltage level under different lightning current crests: down-lead models without corona effect (dashed curves); internal down-lead model with corona effect (red solid curve); external down-lead model with corona effect (blue solid curve); the differences between considering corona effect or not (dot curves).

If the down-lead models consider the corona effect, the reduction on surge impedance leads to the reduction on overvoltage. For both internal down-leads and external down-leads, the overvoltage levels are lower (the absolute levels of the solid curves are lower than the absolute levels of the dashed curves). The differences of overvoltage created by the down-leads considering corona effect or not are also shown. Along with the increasing lightning current, the differences also increase, because higher overvoltage induce thicker corona sheath resulting in larger overvoltage reduction. However, the difference growth rate of the internal down-lead with/without corona is much smaller than that of the external down-lead, especially when lightning current exceeds 80-100 kA. It is because when lightning current is high enough, the corona sheath around the top part of the internal down-lead reaches the inner surface of the cross arm, which barriers the corona from developing further. As a result, corona on external down-lead is much more effective reducing overvoltage levels than on internal down-lead.

C. *Back Flashover Rate of Composite Pylons Installing Internal and External Down-leads*

The back flashover rates provided by internal down-lead and external down-lead considering corona effect or not are calculated and shown in the following Fig. 6.

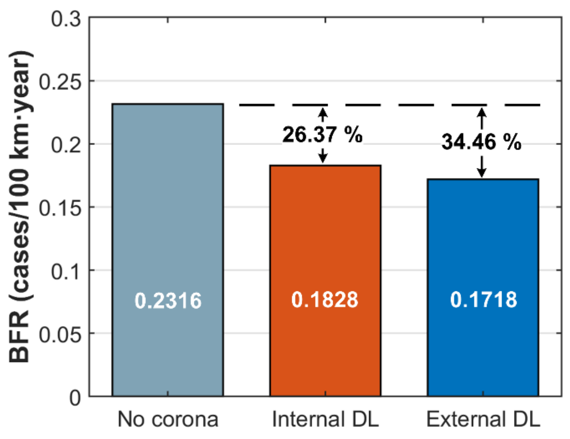

Fig. 6 Back flashover rates: down-lead model without corona effect (grey bar); internal down-lead model with corona effect (red bar); external down-lead model with corona effect (blue bar).

At first, both internal and external down-leads without corona effect give a very close BFR of 0.231 cases per year for a 100-km line, which is respectively 26.37% and 34.46% higher than the BFR provided by internal and external down-lead models considering corona effect. It means that neglecting surge corona effect on thin-wire grounding device can overestimate the severity of back flashover. Secondly, the slightly higher BFR of internal down-lead is due to the cross arm hindering the corona expansion. The barrier of corona happens when lightning current is higher than approximately 80 kA, but the probability of lightning flash with such high current is less than 2.5 %. Thus, the difference between the BFR of composite pylon installing internal and external down-leads is not very notable.

IV. Discussion

A. *Improvement on the Dynamic Corona Modelling*

Based on the above results, the significance of modelling surge corona on the thin-wire grounding devices of composite transmission towers is emphasized. The model can be further improved in the following two factors, dynamic coupling capacitance and surge propagation velocity.

The corona sheath can increase the coupling effect between the down-lead and phase conductors, so that larger coupling capacitance can lower the overvoltage. The corona radius is time-variant and voltage-dependent, so the coupling capacitance should also be.

The corona effect increasing the unit capacitance of the conductors does not only decrease the surge impedance, but it also decreases the surge propagation velocity, as shown in equation (9).

$$v = \frac{1}{\sqrt{LC^*}} \quad [\text{m/s}] \qquad (9)$$

where v is the surge propagation velocity, L is the unit inductance, and C^* is the unit capacitance that varies with corona. The influence of the decrease in propagation velocity is complicated in two contradictory aspects. On the one hand, it attenuates and distorts the surge wave front, which is pushed back so that the steepness of the wave front is decreased. Depending on the wave tail, the crest overvoltage should decrease. On the other hand, it prolongs the time for the reflection wave from the ground potential, which means the crest overvoltage should increase. Thus, the dynamic propagation velocity should be considered in the corona model to make its effect clear.

B. *Suggestions on the Application of the Internal Down-leads for Composite Transmission Towers*

The composite pylon installing internal down-lead is more elegant, which is the original intention of designing aesthetic composite pylons. In order to validate this design, some suggestions are recommended here.

It has been analysed above that surge corona can lower possible overvoltage. The feasibility of a cable through a hollow cross arm as grounding down-lead is investigated in [16]. The insulation layer of the cable hinders the corona inception. Thus, a bare conductor with proper support to make sure it in the middle of cross arm is more desirable.

The cross arm is in a conic shape with a shorter radius at the top and a longer radius at the bottom. However, because the overvoltage rises higher at the top and lower at the bottom, the corona radius also expands longer at the top and shorter at the bottom, which is inverse to the shape of the cross arm. A surge corona radius can reach as long as 20-30 cm. Thus, it is desirable to some extent to reserve enough space for corona expansion when designing other cross arms or composite pylons to improve the lightning protection performance.

V. Conclusions

For an increasing number of transmission tower made of composite materials, a grounding down-lead is necessary to bring ground potential to the shield wires. Internal or external down-leads are options. This paper compares the overvoltage levels and the back flashover performance of adopting these two grounding approaches based on a specific composite pylon design. A dynamic corona model is implemented.

Firstly, the mutual capacitances between the down-leads and phase conductors are simulated and calculated by FEM tools. Without considering the corona, external down-lead has a slightly lower surge impedance and mutual capacitances, but the two grounding approaches give the close back flashover rates.

Secondly, it is stressed that the surge corona effect is necessary for modelling thin-wire grounding devices, otherwise, the back flashover rate can be overestimated by 20% to 30%.

If the corona effect is considered, the back flashover rate provided by adopting internal down-leads is a bit higher, because the corona expansion can be hindered in the cross arm when lightning current is high enough.

References

[1] ENTSO-E. "Ten-Year Network Development Plan 2020. At a glance: Power system needs in 2030 and 2040." https://tyndp.entsoe.eu/ (accessed.

[2] BYSTRUP Design & Engineering. "EUROPEAN COMPOSITE PYLON." https://www.compositepylon.com/ (accessed.

[3] T. K. Sørensen, J. Holbøll, and S. Mikkelsen, "Composite based EHV AC overhead transmission lines," Department of Electrical Engineering, Technical University of Denmark, 2010.

[4] Q. Wang, "Experimental investigation on electrical behaviors of an innovative 400-kV double-circuit composite tower," Department of Energy, Aalborg University, 2018.

[5] P. Salokannel. "T-pylon." https://petterisalokannel.com/RIBA-Competition-T-Pylon-2011 (accessed.

[6] S. M. Musa and M. N. Sadiku, "Application of the finite element method in calculating the capacitance and inductance of multiconductor transmission lines," in *IEEE SoutheastCon 2008*, 2008: IEEE, pp. 300-304."

[7] J. Dias Pinto, A. Paulo Coimbra, P. G. Pereirinha, and C. Lemos Antunes, "Evaluation of the high voltage transmission line inductance and capacitance using the finite element approach," *COMPEL-The international journal for computation and mathematics in electrical and electronic engineering,* vol. 17, no. 3, pp. 313-317, 1998.

[8] H. A. Illias, A. H. A. Bakar, H. Mokhlis, and S. A. Halim, "Calculation of inductance and capacitance in power system transmission lines using finite element analysis method," *Obliczenia indukcyjności i pojemności linii przesyłowej z wykorzystaniem metody elementu skończonego,* vol. 88, no. 10 A, pp. 278-283, 2012.

[9] M. A. Sargent and M. Darveniza, "Tower Surge Impedance," *IEEE Transactions on Power Apparatus and Systems,* vol. PAS-88, no. 5, pp. 680-687, 1969.

[10] M. Ishii *et al.*, "Multistory transmission tower model for lightning surge analysis," *IEEE Transactions on Power Delivery,* vol. 6, no. 3, pp. 1327-1335, 1991.

[11] T. Hara and O. Yamamoto, "Modelling of a transmission tower for lightning-surge analysis," *IEE Proceedings - Generation, Transmission and Distribution,* vol. 143, no. 3, pp. 283-289, 1996.

[12] A. D. Conti, S. Visacro, A. Soares, and M. A. O. Schroeder, "Revision, extension, and validation of Jordan's formula to calculate the surge impedance of vertical conductors," *IEEE Transactions on Electromagnetic Compatibility,* vol. 48, no. 3, pp. 530-536, 2006.

[13] B. Salarieh, H. M. J. D. Silva, A. M. Gole, A. Ametani, and B. Kordi, "An Electromagnetic Model for the Calculation of Tower Surge Impedance Based on Thin Wire Approximation," *IEEE Transactions on Power Delivery,* vol. 36, no. 2, pp. 1173-1182, 2021.

[14] H. Zhang, K. Yin, K. Y. See, Q. Wang, F. F. d. Silva, and C. L. Bak, "A Simplified Dynamic Surge Impedance Model with Corona Effect for Grounding Down-Leads of Composite Pylons," in *2022 36th International Conference on Lightning Protection (ICLP),* 2-7 Oct. 2022 2022, pp. 42-47."

[15] H. Zhang, Q. Wang, K. Yin, C. L. Bak, and F. F. d. Silva, "Transient modelling and backflashover rate analysis of a fully composite pylon," presented at the The 16th IET International Conference on AC and DC Power Transmission (ACDC 2020), 2020."

[16] K. Yin *et al.*, "Feasibility of cable through a hollow cross-arm as down-lead for a 400 kV Y-shaped composite pylon," *Electric Power Systems Research*, vol. 217, p. 109154, 2023/04/01/ 2023.

[17] A. R. Hileman, *Insulation Coordination for Power Systems* (POWER ENGINEERING). Taylor & Francis Group, 1999.

[18] T. Okada, Y. Baba, T. H. Tran, and V. A. Rakov, "On Possible Influence of Corona Discharge on the Propagation Speed of Lightning Surges Along a Tall Grounded Object," *IEEE Transactions on Electromagnetic Compatibility,* vol. 63, no. 1, pp. 172-180, 2021.

[19] M. Ghomi, H. Zhang, C. Leth Bak, F. Faria da Silva, and K. Yin, "Integrated model of transmission tower surge impedance and multilayer grounding system based on full-wave approach," *Electric Power Systems Research,* vol. 198, p. 107355, 2021/09/01/ 2021.

[20] T. Shindo and T. Suzuki, "A New Calculation Method of Breakdown Voltage-Time Characteristics of Long Air Gaps," *IEEE Transactions on Power Apparatus and Systems,* vol. PAS-104, no. 6, pp. 1556-1563, 1985.

[21] CIGRE Working Group C4. 23, "Procedures for Estimating the Lightning Performance of Transmission Lines—New Aspects," *Technical Brochure,* vol. 839, 2021.

[22] K. Yin, M. Ghomi, H. Zhang, C. Leth Bak, F. Faria da Silva, and Q. Wang, "Lightning transient response of bifurcation structure pylon and its empirical expression with high accuracy," *International Journal of Electrical Power & Energy Systems,* vol. 148, p. 108967, 2023/06/01/ 2023.